

Elastic Scattering of 22-Mev Alpha Particles*

N. S. WALL,† J. R. REES, AND K. W. FORD
Indiana University, Bloomington, Indiana

(Received October 15, 1954)

The elastic scattering of 22-Mev alpha particles from silver, gold, and lead has been measured as a function of angle. The differential cross section has been found to follow Rutherford's equation at forward angles but at some critical angle the cross section deviates, first increasing slightly for lead and gold and then decreasing monotonically. The silver distribution shows no increase.

The lead and gold data have been fitted with a modification of Blair's sharp angular momentum cut-off theory but there is no satisfactory agreement between theory and experiment for the silver data. Using this type of analysis one is able to find a nuclear radius that follows the $R=r_0A^{1/3}$ law with $r_0=1.5\times 10^{-13}$ cm only if one assumes a large size, $\sim 2.5\times 10^{-13}$ cm, for the alpha particle.

I. INTRODUCTION

MANY of the earliest experiments which cast light on nuclear size employed alpha particles emitted from naturally radioactive elements and scattered by thin foils of various elements.¹ The angular distribution of scattered particles was compatible with the assumption of a small nucleus exerting a repulsive Coulomb force on the incident alpha particles. These experiments took place about 40 years ago, and the results were sufficient to establish Rutherford's atomic model and give some quantitative information concerning the nuclear radius and nuclear forces.²

Recently, interest has revived in the scattering of alpha particles, because with the cyclotron one can accelerate them to energies sufficient to approach heavy nuclei within the range of nuclear forces. Moreover, we have more intense beams and improved detectors of the scattered particles. Farwell and Wegner³ have measured the energy dependence of elastic alpha-particle scattering for several elements of high atomic number using the 45-Mev alpha beam of the University of Washington cyclotron. The following experiments are complementary to their work in that we have scattered the same particles from some of the same nuclei and investigated the elastic angular distribution in about the same energy range.

To explain the results of Farwell and Wegner, Blair⁴ has made simplifying assumptions concerning the interaction of the alpha particle and the target nucleus. When the apsidal distance of an alpha-particle's classical trajectory is greater than an "interaction radius," he assumes that the particle is elastically scattered with

only a Coulomb phase shift, and when the apsidal distance is less than this "interaction radius," he assumes that the particle is absorbed by the nucleus. The coefficient η_l of the outgoing wave,^{5,6} under these assumptions, is $e^{2i\sigma_l}$ for $l>l'$, where σ_l is the Coulomb phase shift, and is zero, for $l\leq l'$, where l' satisfies the equation,

$$l'(l'+1) = 2mR^2\hbar^{-2}(E - E_c), \quad (1)$$

with

$$E_c = Zze^2R^{-1}; \quad (1')$$

where l' is the orbital angular momentum of a particle of mass m and initial energy E ; E_c is the Coulomb potential energy at the classical turning point; and R is the apsidal distance which is here set equal to the sum of the radii of the nucleus and the alpha particle. Ze is the charge of the target nucleus and ze that of the incident particle; both charge distributions are assumed to be spherically symmetrical.

Under these assumptions,

$$\frac{d\sigma}{d\Omega} = \left| \frac{e^{2i\sigma_0}}{2ik} \left\{ \frac{-in}{\sin^2(\theta/2)} \exp(-in \ln \sin^2 \frac{1}{2}\theta) - \sum_{l=0}^{l'} (2l+1)e^{2i(\sigma_l - \sigma_0)} P_l(\cos\theta) \right\} \right|^2. \quad (2)$$

The Coulomb phases are given by

$$e^{2i\sigma_l} = \Gamma(l+1+in)/\Gamma(l+1-in), \quad (3)$$

and

$$n = zZe^2/\hbar v. \quad (4)$$

The first term in this expression represents the scattering due to the Coulomb potential,⁶ and the second term represents the interaction of the alpha particles with $l\leq l'$ according to Blair.⁴ At small angles, $(\sin \frac{1}{2}\theta)^{-4}$ is large and the scattering is predominately Rutherford scattering unless l' is very large. For alpha

* This work was supported in part by a joint program of the U. S. Office of Naval Research and the U. S. Atomic Energy Commission.

† Now at the University of Rochester, Rochester 3, New York.

¹ In addition to the references on the early elastic scattering of alpha particles given in reference 3 there is a summary of this work in Rutherford, Chadwick, and Ellis, *Radiation from Radioactive Substances* (Cambridge University Press, London, 1930).

² A very complete series of experiments was conducted and interpreted by W. Riezler, Proc. Roy. Soc. (London) **134**, 154 (1932).

³ G. W. Farwell and H. E. Wegner, Phys. Rev. **93**, 356 (1954) and Phys. Rev. **95**, 1212 (1954).

⁴ J. S. Blair, Phys. Rev. **95**, 1218 (1954).

⁵ We use the notation of reference 10 throughout this paper. The Coulomb scattering amplitude however is that given by reference 6.

⁶ N. F. Mott and H. S. W. Massey, *The Theory of Atomic Collisions* (Oxford University Press, London, 1949), second edition, Chap. 3.

particles incident on heavy target nuclei with an initial energy of 22 Mev (the energy of the Indiana University alpha beam), n is found to be about 11, and n' should be less than about 10.

II. EXPERIMENTAL TECHNIQUES

The Indiana University cyclotron produces a 22-Mev alpha-particle beam which passes through a focusing magnet and an analyzing magnet and is brought to a focus on a target in the center of a 15-inch inside diameter scattering chamber associated with the 20-inch double focusing magnetic spectrometer.⁷⁻⁹ A NaI(Tl) scintillation spectrometer for heavy particles has been incorporated into the scattering chamber. The crystal, photomultiplier tube, and preamplifier are mounted within the chamber on an arm which can be rotated in a horizontal plane about an axis passing vertically through the target. A Lucite disk, graduated along its circumference in degrees, is fastened rigidly to the axle of the rotating arm so that the angle of the scintillation counter relative to the beam can be measured with a sensitivity of $\frac{1}{4}$ degree.

In the earliest experiments a Du Mont 6291 multiplier phototube was mounted vertically on the arm with a suitable crystal holder; however, because of the limited dimensions of the scattering chamber and the size of the phototube, the defining aperture of the spectrometer did not move in a plane containing the target. This meant that the angle the spectrometer made with the beam was defined by both a horizontal angle and a vertical angle. We had some difficulty determining the vertical angle, and so, at a sacrifice in resolution, this detector was replaced with one employing a Du Mont type K-1211 miniature photomultiplier situated horizontally in the chamber and rotating in a plane intersecting the target. This counter was aligned vertically with the beam defining slit system by optical means. The resolution of the first detector was 3 percent (full width at half-maximum) for 22-Mev alpha particles elastically scattered from a thin lead target, while that of the second was 8 percent. The lower resolution was attributed to the slightly lower photocathode sensitivity of the K-1211 and to a more compact optical system which resulted in a nonuniform light collection.

The smaller tube made it possible to operate the counter at a smaller minimum angle and thus to show that the small-angle scattering follows the Rutherford formula.

After the installation of the small tube a solid-angle correction as a function of angle was found necessary. A thin thorium alpha-particle source was placed in the target position and the counter was rotated around it. The counting rate varied with the angular position of

⁷ Rasmussen, Miller, Carmichael, and Sampson, Phys. Rev. **92**, 852(A) (1953).

⁸ F. E. Steigert, dissertation, Indiana University, 1953 (unpublished).

⁹ B. M. Carmichael, dissertation, Indiana University, 1954 (unpublished).

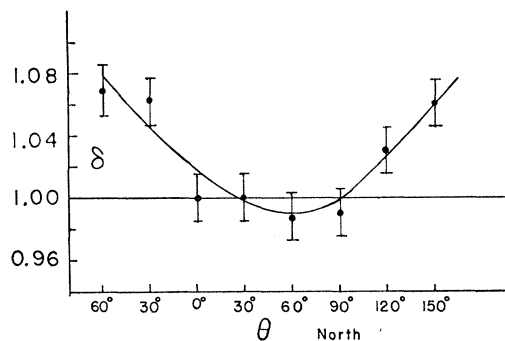


FIG. 1. The correction δ for the effective solid angle as a function of scattering angle.

the counter. Then the source was rotated with the counter fixed and no variation in counting rate was observed. It was concluded that the discrepancy was due to a variation in the solid angle subtended at the source by the counter aperture. Evidently the axis of rotation of the counter did not pass through the center of the target position and the radial distance of the aperture from the source varied with rotation. The effect can be explained if it is assumed that the axis of rotation was displaced 0.1 inch from the center of the target. A plot of the effective solid angle correction as a function of angle is given in Fig. 1. The maximum variation over the range of angles used in these experiments is about 6 percent.

The graduated Lucite disk was positioned arbitrarily on the axis, so it was necessary to determine, experimentally, what reading on the disk corresponded to an angle of zero degrees with respect to the incident beam. This was done by taking a portion of the angular distribution of elastically scattered particles at about 30 degrees on either side of the beam direction. The angles of equal scattered intensity were determined and from them the zero angle. We feel that this measurement is accurate to $\frac{1}{4}$ degree. Figure 1 shows that the effective solid angle is about 5 percent larger in the region of 30 degrees south than on the opposite side of zero; however, this introduces a systematic error of less than $\frac{1}{2}$ degree in the determination of the zero angle. The over-all accuracy of the angle determination then is well within 1 degree. The counter aperture was approximately 1 degree.

The electronic apparatus associated with the spectrometer consisted of a cathode-follower preamplifier mounted on the arm with the photomultiplier tube, an Atomic Instruments Company Model 204-B linear amplifier, a scaler, and power supplies. The high voltage for the photomultiplier was supplied by the Pittsburgh circuit¹⁰ and was monitored by a potentiometer capable of detecting a change of 0.02 percent. This supply was built by Mr. O. E. Johnson of this laboratory.

¹⁰ Progress Report, University of Pittsburgh (unpublished).

The experimental procedure was to count all pulses larger than 85 percent of the pulse height of the elastic group. This was done by adjusting the amplifier's amplitude discriminator to the desired level and counting the discriminator output. Since all of the nuclei investigated were rather heavy and yielded no inelastic groups near the energy of the elastic group, it was found unnecessary to vary the discrimination level as the angle was varied. The level was set at a pulse height corresponding to particles of the energy of those scattered through about 45 degrees, for each element. Such a setting was found to be sufficiently high to discriminate against any elastic alpha particles scattered into back angles by light-weight target contaminants such as carbon or oxygen. At forward angles such particles are only a small fraction of the Coulomb scattered intensity from the heavy nuclei and therefore can be neglected. By displaying the output of the amplifier on an oscilloscope screen and photographing it with a time exposure, the effect of such contaminants in the lead and gold targets was shown to be negligible at back angles. Since the intensity of the alpha-particles scattered by the silver target was quite low, it was difficult to distinguish between silver and contaminant scattering. Thus the silver data presented in Figs. 7 and 8 represent at worst an upper limit.

The cyclotron beam integrator was built and described in detail by Dr. B. M. Carmichael.⁹

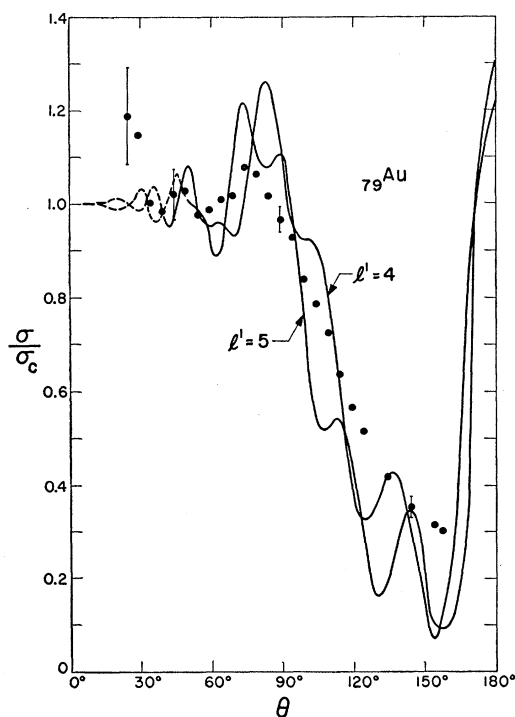


FIG. 2. Scattering of 22-Mev alpha particles by gold. Points are experimental. Curves are theoretical with sharp cut-off model. $n = 10.6$.

The gold and silver targets used were commercially available thin foils. The lead target was prepared by evaporation in vacuum onto a thin film of Zapon.

III. RESULTS

The angular distributions of 22-Mev alpha particles elastically scattered from silver, gold, and lead are given in Figs. 2, 3 (Au); Fig. 4 (Pb); and Figs. 7 and 8 (Ag). The curves in these figures are theoretical, and are discussed in the next section. Figure 5(a) shows the lead and gold data alone. The data have been corrected for the variation in solid angle of acceptance mentioned in the preceding section and plotted in Fig. 1. The angular distribution curves have been normalized arbitrarily in the following manner: the product of the counting rate per unit of charge collected by the Faraday cage and $\sin^4(\frac{1}{2}\theta)$, where θ is the angle of deflection from the beam direction, has been set equal to 1.0 at the forward angles from about 30 degrees to 50 degrees.

The errors indicated in the figures are compounded from the statistical counting errors and errors due to an assumed $\frac{1}{2}$ degree error in the angular position of the counter. The over-all errors are thought to be the same as those indicated except at back angles where they may be somewhat higher due to target contaminants. (See Sec. II.) The data show some deviations from Rutherford scattering at forward angles, but they are not consistent from run to run; it is therefore felt that such discrepancies are purely experimental. The beam is collected in a Faraday cup which may leak charge to the counter framework at the most forward angles. Moreover, at the most forward angles the Coulomb differential cross section is so high that the beam intensity must be kept extremely low and the beam integration may not be accurate. The rise for Pb and Au in the vicinity of 90 degrees, however, is thought to be real inasmuch as it appeared, within one standard deviation for all the runs on these two elements.

The experimental data for Au and Pb show very similar behavior. The cross sections rise to about 10 percent above Coulomb at an angle of 80 to 90 degrees, then fall off smoothly, without any indication of a diffraction pattern, to about 30 percent of Coulomb at the largest angles measured.¹¹ The Ag cross section, which should be influenced by a larger number of partial waves, falls off at a smaller angle, and decreases smoothly to about 1 percent of Coulomb at 135 degrees. For Ag, the experimental errors are too great to detect a 10 percent rise of the cross section before the fall off.

According to Blair's interpretation, the angle corresponding to $\sigma/\sigma_c = \frac{1}{4}$ should give an apsidal distance in agreement with other indications of nuclear size. In these experiments only the silver data drops to $\sigma/\sigma_c = \frac{1}{4}$ and at this angle the interaction distance is calculated to be $(9.1 \pm 0.3) \times 10^{-13}$ cm, in disagreement with

¹¹ Preliminary data taken at angles back to 167 degrees shows no increase in σ/σ_c for Au.

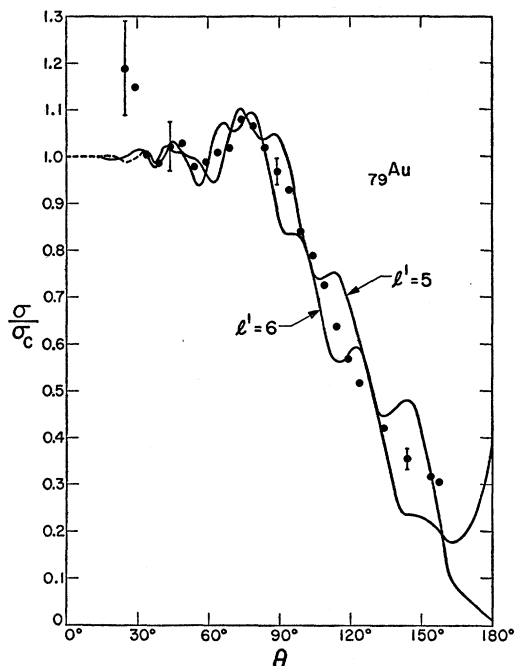


FIG. 3. Scattering of 22-Mev alpha particles by gold. Points are experimental. Curves are theoretical with fuzzy model. $n=10.6$.

Farwell and Wegner's $(8.3 \pm 0.3) \times 10^{-13}$ cm. Further interpretation of the data is given in the next section.

IV. THEORY AND DISCUSSION

The model of Blair, described in Sec. I, has the great merit of simplicity. Because of its rather successful application to the energy dependence of alpha-particle scattering at 60 and 90 degrees, we undertook to use the model to calculate the angular distribution of scattered alpha-particles from gold, lead, and silver, at the fixed energy of this experiment, 22 Mev. A brief discussion of the numerical work is given in an appendix.

(a) Gold

The best fits to the Au data are obtained with $l'=4$ or 5 (Fig. 2), i.e., with partial waves through the fourth or fifth subtracted from the scattered Coulomb wave (for gold, $n=10.6$). The theory reproduces the qualitative features of a rise followed by a sharp fall off of the relative cross section. The rise, however, is to about 20 percent above Coulomb instead of 10 percent, and the theoretical curves show a diffraction pattern, increasing in amplitude with increasing angle. This latter defect of the theory may readily be attributed to the sharp angular momentum cut-off (or, equivalently, radial cut-off) of the Blair model. Most of the ways one might think of to improve the theory, such as the calculation of phase shifts with a complex potential, would increase the difficulties of calculation by orders of magnitude. We therefore altered the theory in the

simplest possible way from the sharp cut-off form into what we shall call the fuzzy Blair model. For $l < l'$, the partial waves are still completely absorbed. For $l > l'$, the partial waves are still unaffected by the nucleus. For $l = l'$, we let the scattered wave have the Coulomb phase and an amplitude of 0.5. This smoothes out somewhat the transition from absorption by the nucleus to no effect by the nucleus, not in a realistic way but in a way which may give qualitative understanding of the deficiencies of the sharp cut-off model. In Fig. 3 are shown the same gold data, and the best fits of the fuzzy model ($l'=5$ or 6). The fit to the data is substantially improved. The theoretical maximum relative cross section is now 1.1, in agreement with the experiment, the diffraction pattern is somewhat damped out, and the experimental points between 90 and 150 degrees are followed more closely. From this agreement it seems reasonable to conclude that the first few partial waves are indeed strongly absorbed (from the elastic beam) and that the transition from strong absorption to no absorption occurs over only a few partial waves. The spread in energy of the incident beam of about 0.1 Mev is not sufficient to account for lack of diffraction effects in the experimental results. For Pb and Au, a spread of 0.5 Mev and for Ag a spread of greater than 1 Mev would be required to smooth out the theoretical diffraction effects.

(b) Lead

The remarks above concerning gold apply equally well to lead (for lead, $n=11.0$). For lead also, the fuzzy model gives a substantially improved fit to the data over the sharp cut-off model. In Fig. 4 are shown the

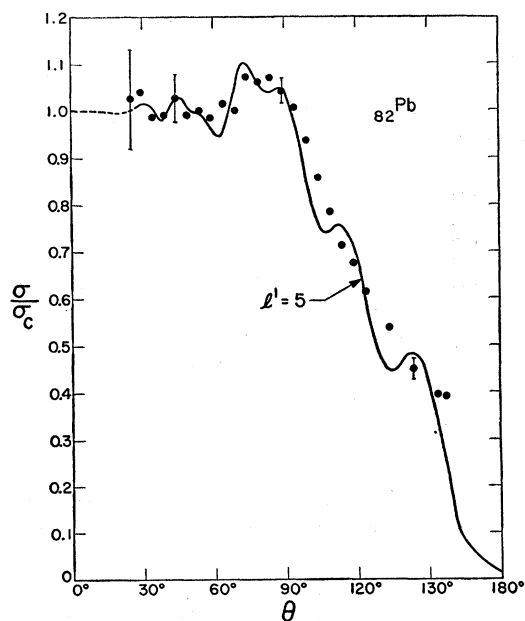


FIG. 4. Scattering of 22-Mev alpha particles by lead. Points are experimental. Curve is theoretical with fuzzy model (and $n=10.6$ instead of 11.0).

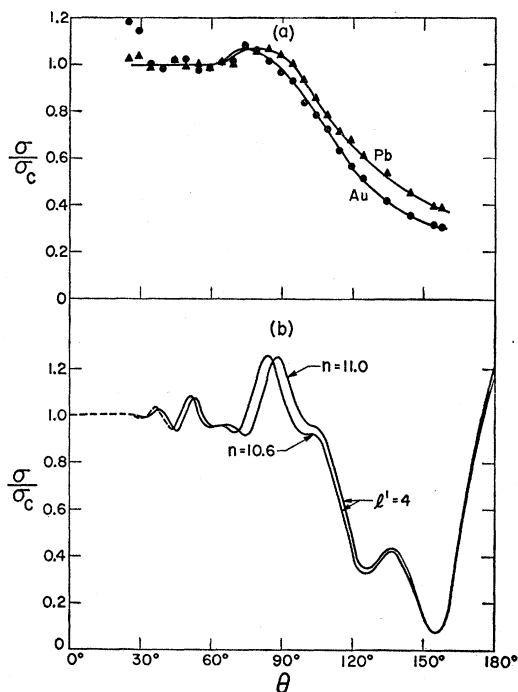


FIG. 5. (a) Gold and lead angular distributions compared. Curves drawn through data are not theoretical. (b) Theoretical cross sections for sharp cut-off model compared at fixed l' for the values of n corresponding to gold and lead.

lead data, together with the best fit—the fuzzy model with $l'=5$, but with $n=10.6$. Because of the small difference in the n -values of Au and Pb, the cross sections for the fuzzy model were calculated for only one of them. [See Fig. 5(b) for the effect of changing n from 10.6 to 11 for a fixed l' .]

(c) Gold vs Lead

For both gold and lead separately, values for the “interaction radius” may be obtained [part (e)]. Be-

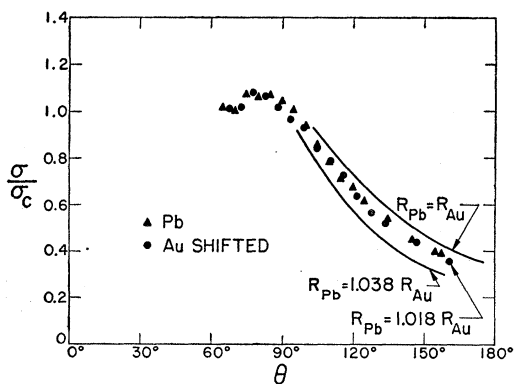


FIG. 6. Determination of relative radii of gold and lead. The gold data are shifted according to the classical arguments of the text into near coincidence with the lead data with $R_{Pb}=1.018 R_{Au}$. For two other choices of relative radii, the loci of the shifted gold points are shown by solid curves.

cause of the similarity of the cross sections, however, one can learn in more detail the *relative* size of the gold and lead nuclei. For comparison, the gold and lead data are shown on the same graph, Fig. 5(a). (The curves are drawn through the points, and are not theoretical.) Figure 5(b) gives theoretical curves for $n=10.6$ (gold) and $n=11.0$ (lead) for the same value of l' . These justify the use of $n=10.6$ to fit the lead data in Fig. 4, and also show that the gold-lead difference of Fig. 5(a) is greater than can be accounted for by the different Z (or n) values for given l' .

In order to interpret the difference of the gold and lead cross sections, we turn to a wholly classical picture. We suppose that the ratio of the cross section to the Coulomb cross section depends only on the distance of the point of closest approach from the nuclear surface. Let the alpha particle scattered from element Z_i through angle θ_i have a classical apsidal distance $r_{\min}(i)$. Then our supposition is

$$\sigma_1(\theta_1)/\sigma_c(\theta_1) = \sigma_2(\theta_2)/\sigma_c(\theta_2),$$

if

$$r_{\min}(1) - R_1 = r_{\min}(2) - R_2.$$

TABLE I. Determination of difference of radii of Pb and Au nuclei. $\delta R = R_{Pb} - R_{Au}$ in units of 10^{-13} cm. θ_{Au} = angle of scattering from Au nucleus. θ_{Pb} = angle of scattering from Pb nucleus for which the relative cross section is equal to that of Au at θ_{Au} . $\delta\theta = \theta_{Pb} - \theta_{Au}$. All angles in degrees.

| θ_{Au} | $\delta\theta_{exp}$ | $\delta\theta_{theoretical}$ | | | |
|---------------|----------------------|------------------------------|-----------------|-----------------|-----------------|
| | | $\delta R=0$ | $\delta R=0.10$ | $\delta R=0.15$ | $\delta R=0.20$ |
| 90 | 6 ± 1 | 8 | 6 | 5 | 4 |
| 100 | 5 ± 1 | 19 | 7 | 6 | 5 |
| 110 | 7 ± 1 | 13 | 9 | 8 | 6 |
| 120 | 10 ± 1 | 17 | 12 | 10 | 8 |
| 130 | 15 ± 1 | 24 | 16 | 13 | 10 |
| 140 | 19 ± 1 | ... | 28 | 19 | 14 |

This is analogous to Blair's more specific assumption that the relative cross section, σ/σ_c , should be equal to $\frac{1}{4}$ when the classical apsidal distance is equal to the nuclear radius. Our generalization rests on the same physical idea, that for this semiclassical problem ($n \gg 1$), one can think of the alpha particle as a rather well-defined wave packet sweeping by the nucleus.

The classical formula for the point of closest approach, r_{\min} , is

$$\hbar^{-1} p r_{\min} = n \cot^2 \frac{1}{2} \theta / (\csc \frac{1}{2} \theta - 1) \equiv n f(\theta),$$

where p is the incident momentum, and n is defined by (4). Our supposition about relative intensities then leads to

$$n_2 f(\theta_2) = n_1 f(\theta_1) + \hbar^{-1} p (R_2 - R_1), \quad (5)$$

where θ_1 and θ_2 are the angles for which the cross sections of elements 1 and 2 (relative to Coulomb) are equal. For a given assumption about $R_{Pb} - R_{Au}$, we solve Eq. (5) for θ_{Pb} , the angle where the Pb cross section should be equal to the Au cross section at θ_{Au} . A sum-

mary of these calculations is given in Table I. From the best fit obtained for $\theta_{\text{Pb}} - \theta_{\text{Au}}$ as a function of θ_{Au} , we conclude

$$R_{\text{Pb}} - R_{\text{Au}} = (0.15 \pm 0.05) \times 10^{-13} \text{ cm.}$$

This difference is consistent with $R = 1.5 \times 10^{-13} A^{1/3}$ cm; it shows that the radius of Pb exceeds that of gold by a normal amount in spite of the closed shell character of Pb.

A slight variation in this method can be used to obtain a figure for the ratio of the radii of Pb and Au. For classical orbits not far from the nuclear surface, relative cross section for neighboring elements will be nearly equal when

$$r_{\text{min}}(1)/R_1 = r_{\text{min}}(2)/R_2.$$

With this assumption, Eq. (5) is replaced by

$$n_2 f(\theta_2) = (R_2/R_1) n_1 f(\theta_1). \quad (5)'$$

Now each assumption for the ratio, $R_{\text{Pb}}/R_{\text{Au}}$, will lead to a predicted angular shift, $\theta_{\text{Pb}} - \theta_{\text{Au}}$, between the two cross section curves. In Fig. 6 are shown the lead data,

TABLE II. Nuclear radii. All radii in units 10^{-13} cm. $R + R_\alpha$ = interaction radius determined by experiment = $R_0 A^{1/3}$. $R = (R + R_\alpha) - 2.5 \times 10^{-13}$ cm = $r_0 A^{1/3}$.

| Element | l' | $R + R_\alpha$ | R_0 | R | r_0 |
|---------|-----------|----------------|-------|-----|-------|
| Pb | 5 | 11.4 | 1.92 | 8.9 | 1.50 |
| Au | 5.5 | 11.1 | 1.90 | 8.6 | 1.48 |
| Ag | ~ 12 | 9.9 | 1.97 | 7.4 | 1.5 |

and the gold data shifted according to this prescription for several assumptions about $R_{\text{Pb}}/R_{\text{Au}}$. The best overlap between the lead data and the shifted gold data leads to

$$R_{\text{Pb}}/R_{\text{Au}} = 1.020 \pm 0.007,$$

which is consistent with an $A^{1/3}$ law of radii and with the result for the difference of radii.

(d) Silver

The silver data, together with the best fit of the sharp cut-off model, are shown in Fig. 7 (for Ag, $n=6.3$). The agreement between theory and experiment is fair below about 70 degrees, and poor above this angle, with only the minima of a very marked diffraction pattern coming close to the experimental points. With a larger number of partial waves being affected by the nucleus, and with a probably more gradual transition from large to small absorption, it is to be expected that the sharp cut-off model will be less satisfactory. The fuzzy model, however, which is fit to the Ag data in Fig. 8, is not very much better. The theoretical curve follows the points reasonably well to about 85 degrees, then diverges sharply into a diffraction pattern which is broadened relative to that of the sharp cut-off model, but not reduced in amplitude. Thus a very considerably refined model will probably be required to fit the large

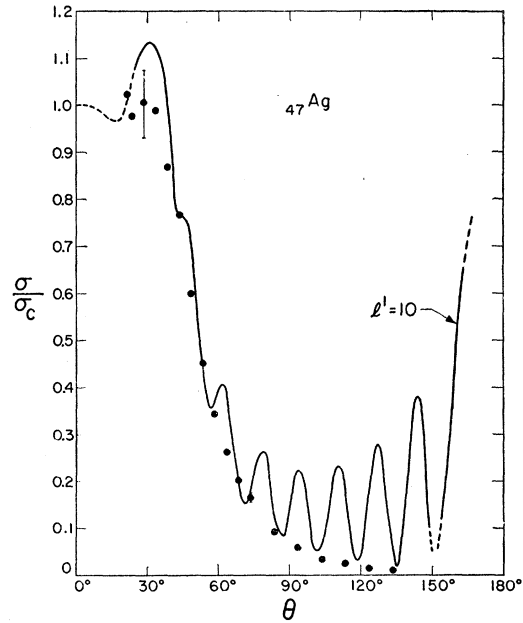


FIG. 7. Scattering of 22-Mev alpha particles by silver. Points are experimental. Curve is theoretical with sharp cut-off model. $n=6.3$.

angle data, which show no evidence at all of a diffraction pattern. A change from an infinite to a finite absorption coefficient of the nucleus may be sufficient to damp out the diffraction pattern, although it seems likely that in addition some account must also be taken of the finite thickness of the nuclear surface in order to explain the complete absence of oscillation in the experimental cross section.

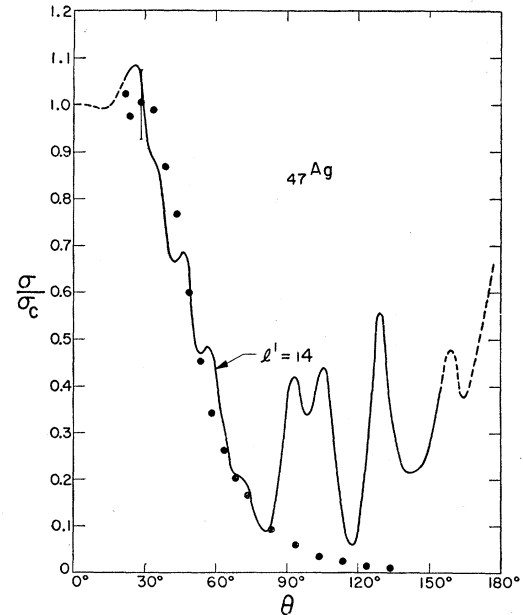


FIG. 8. Scattering of 22-Mev alpha particle by silver. Points are experimental. Curve is theoretical with fuzzy model. $n=6.3$.

(e) Nuclear Radii

The assumption described in Sec. I, and expressed in Eq. (1), that at the critical angular momentum l' , the Coulomb barrier plus the centrifugal barrier at the "interaction radius" is equal to the incident energy, allows one to compute values of the interaction radii for the three nuclei studied. These radii, written as $R+R_\alpha$, are given in Table II. Other radial constants given in Table II are defined as follows. $R_0=(R+R_\alpha)/A^{1/3}$. These values are large compared to alpha-decay radii and very large compared to electromagnetic radii. If we make a generous allowance of 2.5×10^{-13} cm for R_α , we obtain the values of nuclear radius R , and of $r_0=R/A^{1/3}$, given in the last two columns of Table II. This correction brings the value of r_0 down to 1.5×10^{-13} cm. These radii of course depend on the model employed to fit the data, but the general conclusion can be drawn that the nuclear interaction radius is very considerably larger than the electromagnetic radius. It should be mentioned that some evidence for a large alpha-particle radius exists, based upon the experiments of Bashkin^{12,13} and Adair.¹⁴

Finally, we remark that Blair's success in fitting the energy dependence of elastic alpha scattering was to some degree dependent on the particular angles used, 60 and 90 degrees. In Fig. 9, we plot, for $n=10.6$, the relative cross section as a function of the number of partial waves absorbed for several angles. The angle 90 degrees (for all n) has the special property of showing

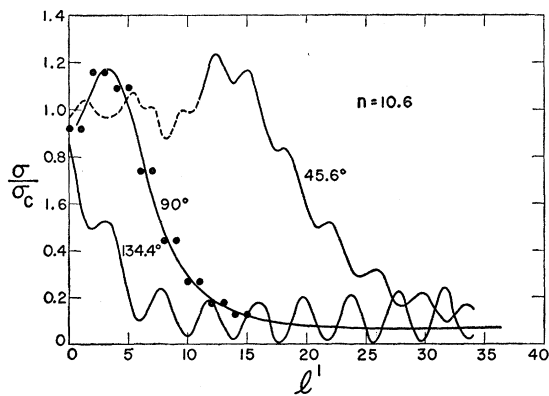


FIG. 9. Relative cross sections vs l' , the number of partial waves absorbed, according to the sharp cut-off model, for several angles.

¹² J. M. Blatt and V. F. Weisskopf, *Theoretical Nuclear Physics* (John Wiley and Sons, Inc., New York, 1952).

¹³ Bashkin, Mooring, and Petree, *Phys. Rev.* **82**, 378 (1951).

¹⁴ R. K. Adair, *Phys. Rev.* **86**, 155 (1952).

no oscillations at large l' . The angle 60 degrees (and other angles less than 90 degrees) shows only a weak oscillation. Angles greater than 90 degrees, here illustrated with 135 degrees, show marked oscillations. It is probable that the model would fail to account for the energy dependence of the scattering at large angles and high energy in the same way that it here fails to account for the angular distribution at larger angles and high l' .

The success of this simple model, especially in its fuzzy form, at fitting the gold and lead data suggests that it might be fruitful to analyze in a similar way angular distributions at other energies at and just above the Coulomb barrier.

ACKNOWLEDGMENTS

The authors would like to acknowledge the valuable assistance of Professor D. W. Miller and Professor M. B. Sampson in conducting these experiments; and we would like particularly to thank Professor V. K. Rasmussen for many interesting discussions and for considerable assistance in setting up the instrumentation involved in these experiments, as well as help in the accumulation of the data.

Professor G. S. Blair, Professor G. Farwell, and Dr. H. Wegner were very generous in supplying us with their data and interpretations prior to publication.

We express our appreciation to Dr. Norris Bradbury and Dr. Carson Mark for the opportunity to carry out a part of this work at the Los Alamos Scientific Laboratory.

APPENDIX—NUMERICAL CALCULATIONS

The ratio σ/σ_c was calculated by means of Eq. (2), with a suitable alteration for the fuzzy model. Since the ratio σ/σ_c was calculated directly, it was unnecessary to find the Coulomb phases σ_l , but only the differences, $\sigma_l - \sigma_0$, given by the recursion formula,

$$e^{2i(\sigma_l - \sigma_0)} = [(l+in)/(l-in)]e^{2i(\sigma_{l-1} - \sigma_0)}.$$

For a given value of n (6.3, 10.6, or 11.0) and a given model (sharp or fuzzy), the ratios σ/σ_c were calculated for all l' from 0 to some maximum, variously taken between 15 and 35, and for 40 equally spaced values of $\cos\theta$ between 0.05 and -1.00 . The calculations were performed on an IBM 701 computer at the Los Alamos Scientific Laboratory, and were greatly simplified by the use of standard programs developed by Los Alamos Group T-1. The calculation of an angular distribution at given n and l' required several seconds.